$$\delta = 1/\lambda_\dagger^*, \qquad \delta_p = 0, \qquad C_f = \lambda_\dagger^* \tag{18}$$

where

$$\lambda_\dagger^* = K + \sqrt{K^2 + M^2}; \qquad K = r_v/2$$

Equation (17a) is the single-phase asymptotic suction profile in the presence of a uniform transverse magnetic field. This solution is consistent with that reported by Singh.[7]

When $\alpha \to \infty$ (equilibrium flow), both phases move together with the same velocity. For this case, Eqs. (14) and (16) can be expressed as

$$F = 1 - \exp(-\lambda_\dagger^{**}\eta) \tag{19a}$$

$$F_p = 1 \tag{19b}$$

$$\delta = \delta_p = 1/\lambda_\dagger^{**}, \qquad C_f = \lambda_\dagger^{**} \tag{20}$$

where

$$\lambda_\dagger^{**} = K(1+\kappa) + \sqrt{K^2(1+\kappa)^2 + M^2} \tag{21}$$

Equation (19a) can be thought of as the asymptotic suction profile in the presence of a uniform transverse magnetic field for a single fluid having density $(1+\kappa)\rho = \rho + \rho_p$.

When $\kappa \to 0$ (dilute limit), the behavior of the fluid phase becomes independent of the presence of particles. As mentioned by Soo,[14] this is the simplest nontrivial case of dispersed two-phase flow. Upon equating $\kappa = 0$ in Eqs. (14) and (16), the corresponding solutions assume the forms

$$F = 1 - \exp(-\lambda_\dagger^*\eta), \qquad F_p = 1 - \alpha/(\alpha + r_v\lambda_\dagger^*)\exp(-\lambda_\dagger^*\eta) \tag{22}$$

$$\delta = 1/\lambda_\dagger^*, \quad \delta_p = \alpha/[\lambda_\dagger^*(\alpha + r_v\lambda_\dagger^*)], \quad C_f = \lambda_\dagger^* \tag{23}$$

It should be mentioned that all of the solutions obtained in the present Note reduce to the results reported by Chamkha and Peddieson[12] if M is equated to zero.

The main purpose of this Note is to show the influence of the magnetic field on the flow properties. This can be seen from Figs. 1-3.

Figures 1-3 present the fluid-phase displacement thickness δ, the particle-phase displacement thickness δ_p, and the fluid-phase skin-friction coefficient C_f vs the inverse Stokes number α for various values of the Hartmann number M, respectively. It can be seen easily from these figures that increases in the Hartmann number M cause increases in the skin-friction coefficient C_f and decreases in the displacement thicknesses for both the fluid and particulate phases δ and δ_p, respectively. The dotted lines correspond to the equilibrium limit.

Conclusions

In the present Note, closed-form solutions for the hydromagnetic flow of a particulate suspension past an infinite porous flat plate were obtained. Some limiting solutions were developed for special cases. Graphical results of the exact solutions were presented and used to show the influence of the presence of a magnetic field on the flow properties. It was concluded that the skin-friction coefficient for the fluid phase increases whereas the displacement thicknesses for both the fluid and particulate phases decrease as the strength of the magnetic field increases.

References

[1]Rossow, V. J., "On Flow of Electrically Conducting Fluids Over a Flat Plate in the Presence of a Transverse Magnetic Field," NACA TN-3971, May 1957.

[2]Kakutani, T., "Effect of Transverse Magnetic Field on the Flow due to an Oscillating Flat Plate," *Journal of the Physical Society of Japan*, Vol. 13, No. 12, 1958, pp. 1504-1509.

[3]Ong, R. S., and Nicholls, J. A., " On the Flow of a Hydromagnetic Fluid Near an Oscillating Flat Plate," *Journal of Aero/Space Sciences*, Vol. 26, May 1959, pp. 313-314.

[4]Gupta, A. S., "On the Flow of an Electrically Conducting Fluid Near an Accelerated Plate in the Presence of a Magnetic Field," *Journal of the Physical Society of Japan*, Vol. 15, No. 10, 1960, pp. 1894-1897.

[5]Suryaprakasarao, U., "The Response of Laminar Skin Friction, Temperature and Heat Transfer to Fluctuations in the Stream Velocity in the Presence of a Transverse Magnetic Field I," *Zeitschrift fuer Angewandte Mathematik und Mechanik*, Vol. 42, 1962, pp. 133-141.

[6]Muhuri, P. K., "Flow Formation in Couette Motion in Magnetohydrodynamics with Suction," *Journal of the Physical Society of Japan*, Vol. 18, No. 11, 1963, pp. 1671-1685.

[7]Singh, D., "Hydromagnetic Flow Illustrating the Response of a Laminar Boundary Layer to a Given Change in the Free Stream Velocity," *Journal of the Physical Society of Japan*, Vol. 18, No. 11, 1963, pp. 1676-1785.

[8]Baral, M. C., "Plane Parallel Flow of a Conducting Dusty Gas," *Journal of the Physical Society of Japan*, Vol. 25, No. 6, 1968, pp. 1701-1702.

[9]Ramana Rao, V. V., "A Note on Plane Parallel Flow of Conducting Dusty Gas-II," *Journal of the Physical Society of Japan*, Vol. 34, 1973, p. 843.

[10]Dube, S. N., and Sharma, C. L., "A Note on Unsteady Flow of a Dusty Viscous Liquid in a Channel Bounded by Two Parallel Flat Plates," *Journal of the Physical Society of Japan*, Vol. 38, 1975, p. 297.

[11]Mitra, P., and Bhattacharyya, P., "On the Hydromagnetic Flow of a Dusty Fluid Between Two Parallel Plates, One Being Stationary and the Other Oscillating," *Journal of the Physical Society of Japan*, Vol. 50, No. 3, 1981, pp. 995-1001.

[12]Chamkha, A. J., and Peddieson, J., "Exact Solution of the Two-Phase Asymptotic Suction Profile," *Developments in Theoretical and Applied Mechanics*, Vol. 14, 1988, pp. 215-222.

[13]Marble, F. E., "Dynamics of Dustry Gases,"*Annual Reviews of Fluid Mechanics*, Vol. 2, 1970, pp. 397-446.

[14]Soo, S. L., "Development of Theories of Liquid-Solid Flows," *Journal of Pipelines*, Vol. 4, 1984, pp. 137-142.

Vibration Mode Shape Control by Prestressing

Jan Holnicki-Szulc*
Polish Academy of Sciences, 00-049 Warsaw, Poland
and
Raphael T. Haftka†
Virginia Polytechnic Institute and State University, Blacksburg, Virginia 24061

Introduction

In many applications we have points on a structure that need to be protected from excessive vibration. A common example is that of a car where the designer attempts to have low vibration amplitudes under the driver's seat. In the case of large space structures, the position of sensitive instruments is expected to dictate the need for such vibration protection at selected points. In the present Note we are concerned with excitation in a narrow frequency band, so that only a small number of vibration modes contribute to the intensity of the forced response. In many cases it is not feasible to move the natural vibration frequencies of the structure far enough from this excitation band, so that we need to consider instead the expedient of reshaping the vibration modes to reduce the amplitude of vibration at the critical point or points.

Received March 9, 1991; revision received Sept. 13, 1991; accepted for publication Oct. 14, 1991.

*Associate Professor, Institute of Fundamental Technological Research, Swietokrzyska 21.

†Professor, Aerospace and Ocean Engineering Department.

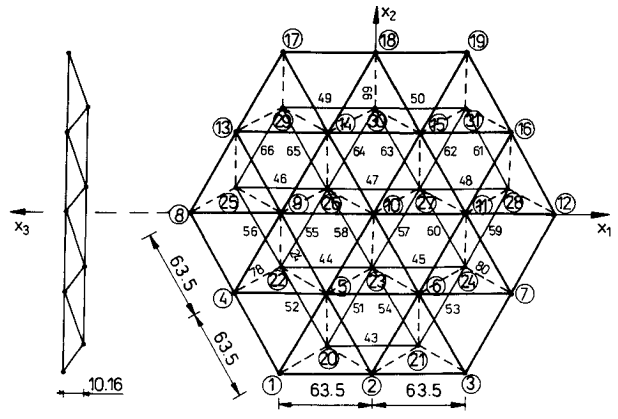

Fig. 1 Antenna truss structure.

The process of shaping the modes of a structure to reduce the forced response can take two routes. If the shape of excitation is known (at least approximately), we can attempt to make the mode shapes orthogonal to the excitation.[1,2] In the present Note we discuss the second route of reshaping the modes so that their amplitude is small at a desired point. If possible, it would be desirable to move the nodal lines of the modes to pass through the desired point.[3] However, in most situations it is not possible to do that with more than one mode.

Recently, there has been much interest in the use of piezoelectric actuators for vibration damping in large space structures.[4,5] If such devices are to be used, it makes sense to employ them also for the shaping of the vibration modes affecting sensitive points on the structure. The present Note explores this approach.

Problem Formulation

We consider the vibration eigenproblem

$$(K-\lambda M)u=0 \tag{1}$$

where K and M are the stiffness and mass matrices, respectively, λ is the vibration eigenvalue (equal to the square of the frequency ω), and u is the vibration mode normalized as follows:

$$u^TMu=1 \tag{2}$$

The stiffness matrix in a structure with some prestress is given as

$$K=K_0+K_G \tag{3}$$

where K_0 is the stiffness matrix of the unloaded structure and K_G the geometric (differential) stiffness matrix. The geometric stiffness matrix depends on the geometry of the elements and on the state of internal forces. For example, it accounts for the fact that the lateral vibration of a beam is reduced when the beam is in a state of axial compression.

In this Note, we are interested in the use of piezoelectric actuators in large truss structures that introduce initial distortions ϵ_0. Therefore, the vibration modes depend on the initial distortions. We assume that the response of the structure is governed by a narrow-band excitation in the vicinity of a frequency ω_0 and that r vibration frequencies are close enough to ω_0 so that the corresponding modes are substantially excited by the disturbance. That is, denoting these frequencies by ω_i, $i=1,\ldots,r$ we have

$$|\omega_i/\omega_0|-1\ll 1 \tag{4}$$

For any vibration mode, we are interested in reducing the magnitude of a linear functional u_l of the mode

$$u_l=e^Tu \tag{5}$$

where e is a vector. In the examples in this Note, u_l is the value of a component of the mode at a given point on a truss structure. In that case, the vector e is all zeroes except for the desired component, which is one.

We consider first the case when the frequencies are exactly the same, so that any linear combination of the modes

$$u=\sum_{i=1}^{r}\alpha_iu_i \tag{6}$$

is also a mode. The normalization condition, Eq. (2), leads to

$$\sum_{i=1}^{r}\alpha_i^2=1 \tag{7}$$

Our measure of the severity of the vibration is the maximum value u_{lm} of u_l obtained over all possible values of the various α_i. That is,

$$u_{lm}=\max_{\alpha i}\sum_{i=1}^{r}\alpha_ie^Tu_i$$

such that (8)

$$\sum_{i=1}^{r}\alpha_i^2=1$$

The solution to this maximization problem is

$$\alpha_i=e^Tu_i/\mu \tag{9}$$

where μ is given as

$$\mu=\left[\sum_{i=1}^{r}(e^Tu_i)^2\right]^{1/2} \tag{10}$$

For the case of closely spaced frequencies, we assume that it is still reasonable to use the same u_{lm} as a measure of the severity of vibration.

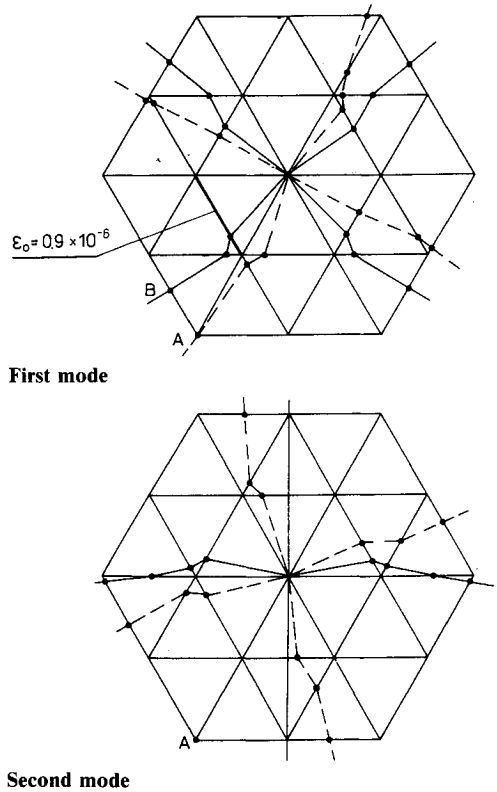

a) First mode

b) Second mode

——— initial configuration ($\lambda_1=\lambda_2=433.135$ (rad/sec)²)
– – – final configuration ($\lambda_1\simeq\lambda_2=433.136$ (rad/sec)²)

Fig. 2 Nodal lines in the case of one mode controlled.

Optimization Procedure

We assume that distortions can be generated only in a defined subset $\mathfrak{C}$ of elements and that the maximum values of the distortions are constrained as

$$|\epsilon_0| \leq \epsilon_m \tag{11}$$

Our optimization problem is defined as the minimization of the objective function, Eq. (8), subject to the constraints of Eq. (11). It is possible to solve this problem using standard optimization programs (e.g., NEWSUMT-A, Ref. 7). However, for the present problem, the constraints of Eq. (11) are simple bound constraints, and the cost of calculating derivatives is comparable to the cost of evaluating the objective function. Therefore, it is reasonable to use a method that calculates these derivatives frequently. The optimization problem leads to the following optimality criterion:

$$\frac{\partial u_{lm}}{\partial \epsilon_0}(\epsilon_0) = \eta_1 - \eta_2 \tag{12}$$

where $\eta_i \geq 0$ $(i = 1, 2)$ are the Lagrange multiplier vectors for the constraints $\epsilon_0 - \epsilon_m \leq 0$ and $\epsilon_0 + \epsilon_m \geq 0$, respectively, and $\partial u_{lm}/\partial \epsilon_0$ is a vector of derivatives with respect to the components of ϵ_0. The optimization procedure can be based on an iterative process using a simple recursion formula:

$$\epsilon_0^{k+1} = \epsilon_0^k - \Delta s\, D^k/(\Sigma D^k)^{1/2}$$

$$\text{if } (\epsilon_0^{k+1} > \epsilon_m), \quad \epsilon_0^{k+1} = \epsilon_m \tag{13}$$

$$\text{if } (\epsilon_0^{k+1} < -\epsilon_m), \quad \epsilon_0^{k+1} = -\epsilon_m$$

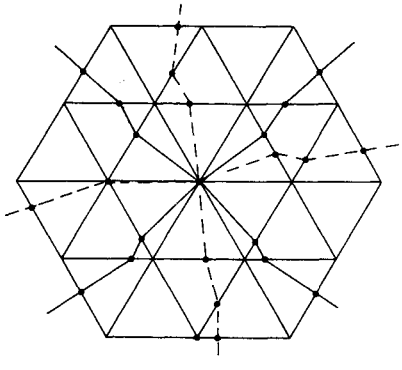

a) First mode

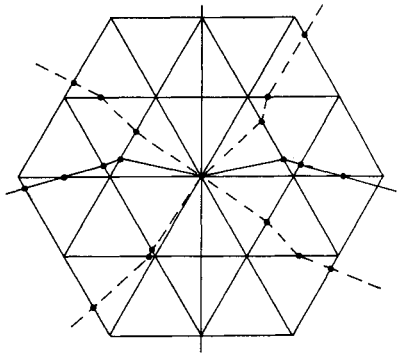

b) Second mode

——— initial configuration ($\lambda_1 = \lambda_2 = 433.135$ (rad/sec)^2)
– – – final configuration ($\lambda_1 \approx 418.9$ (rad/sec)^2)
($\lambda_2 \approx 425.4$ (rad/sec)^2)

Fig. 3 Nodal lines in the case of two modes controlled.

Table 1 Optimal prestress for the antenna truss structure

No.	ϵ_0	$\partial U_{lm}/\partial \epsilon_0$
43	−0.004	0.34
44	0.004	−1.93
45	0.004	−2.87
46	−0.004	0.44
47	−0.004	2.89
48	−0.004	0.57
49	0.003	0.00
50	−0.004	0.75
51	0.004	−0.35
52	−0.003	0.00
53	−0.004	0.71
54	0.004	−0.35
55	−0.004	1.93
56	0.004	−0.69
57	0.004	−1.02
58	0.004	−1.20
59	0.004	−1.88
60	−0.004	2.87
61	0.004	−0.57
62	−0.004	0.57
63	0.004	−0.49
64	−0.004	0.49
65	−0.004	0.44
66	0.004	−0.44

for the distortions from all elements from the subset $\mathfrak{C}$. Here D^k denotes the vector $\partial u_{lm}/\partial \epsilon_0$. and Δs denotes a controlled step size. By using a small step size, the iteration procedure leads smoothly to the optimal solution. For the results described in the next section, derivatives were calculated by finite differences.

Local Reduction of Vibration in a Large Antenna Truss Structure

As an example, we consider the minimization of transverse vibration (in direction x_3) of node 1 of the antenna backup truss structure shown in Fig. 1.

The number of truss elements is 102, and with 31 joints the number of degrees of freedom for all joints is 93. Reducing this number by 6 global degrees of freedom, the structure is 15 times $(102 - 93 + 6 = 15)$ redundant, so that at most 15 linearly independent states of residual forces can be generated. Additionally, it was checked numerically that elements 78, 80, and 99 are isostatic. That is, distortions applied to these elements do not cause residual forces in the structure. Therefore, only 12 linearly independent states of residual forces can be generated in this structure. Therefore, if all members can have actuators, we could search for the optimal prestress considering only 12 independent components (linear combinations of initial distortions imposed on all members) of the solution. However, a more realistic solution should assume a limited number of locations for the actuators.

The truss is made of aluminum with Young's modulus $E = 0.7 \times 10^6$ kg/cm^2 and weight density $\rho = 0.027$ kg/cm^3. The cross-sectional area of the elements is $F = 6.45$ cm^2, and the limit values of the distortion are $\epsilon_m = 0.004$. The structure without any prestress has been treated as the starting configuration for the optimization procedure. For this configuration the lowest eigenvalue is repeated twice, $\lambda_1 = \lambda_2 = 433.135$ (rad/s)^2. The nodal lines for the first two modes of vibration are shown in Figs. 2a and 2b, respectively (continuous lines). Only the upper layer of the truss structure and the distribution of vertical components (parallel to x_3) of eigenvectors are shown in Fig. 2. Restricting our considerations to these two modes $(r = 2)$, the objective function in Eq. (8) takes the value $u_{lm} = 1.0808$.

The sensitivity of modal lines position for a chosen mode is very high in the case of multiple eigenvalues. For example, it was checked that the small distortion $\epsilon_0 = 0.9 \times 10^{-6}$ introduced only into element no. 24 reduces the local vibration due to the first mode (assuming $r = 1$) almost to zero. The corresponding nodal lines for the first two modes of vibration are shown in Figs. 2a and 2b, respectively (broken lines). As we can see, the effect of the shifting of the nodal line for the chosen mode (point B) to a certain point (point A) can be done easily.

Of course, the problem of simultaneous reduction of local vibration for the first two modes cannot be so effective. Assuming $r = 2$ and restricting considerations to the set $\mathfrak{A}$ of members from the lower layer (24 elements, nos. 43–66, cf. Fig. 1) as possible locations for actuators, the following optimal solution minimizing the objective function of Eq. (8) has been reached by the optimization procedure, with distortions in elements 43–66, respectively, given in the first row (denoted by ϵ_0) in Table 1.

The objective function was reduced to $u_{lm} = 0.9204$ (local vibration reduced by 15%). The nodal lines for two of the first, optimally shaped modes of vibration are shown (broken lines) in Figs. 3a and 3b, respectively. The gradient of goal function of Eq. (8) (calculated for the preceding solution) with respect to the control parameters takes the components shown in the second row (denoted by $\partial u_{lm}/\partial \epsilon_0$) in Table 1.

The products of the components of vectors ϵ_0 and $\partial u_{lm}/\partial \epsilon_0$ (a component-by-component check) take nonpositive values (with zero values for unconstrained components), so it can be proved that the Kuhn-Tucker stationary conditions are satisfied for the solution.

Concluding Remarks

A procedure for reducing vibration at sensitive locations on a structure by induced distortions was derived and demonstrated for an antenna truss example. It was shown that with repeated frequencies it is very easy to move nodal lines of one of the modes. For the more realistic problem of modifying both modes, it was still possible to obtain 15% reduction in amplitude with induced distortions limited to 0.4%.

In real applications an additional constraint may be to reduce the number of elements that contain length actuators. In such a case it may be important to locate the most effective elements first before proceeding to the optimization of the values of the induced distortions.

Acknowledgment

This work was supported in part by NASA Grant NAG-1-224.

References

[1]Taylor, R. B., "Helicopter Vibration Reduction by Rotor Blade Model Shaping," 38th Annual Forum of the American Helicopter Society, Paper A-82-38-09-3000, Anaheim, CA, May 1982.

[2]Taylor, R. B., "Helicopter Rotor Blade Design for Minimum Vibration," NASA CR-3825, Oct. 1984.

[3]Pritchard, J. I., Adelman, H. M., and Haftka, R. T., "Sensitivity Analyses and Optimization of Nodal Point Placement for Vibration Reduction," NASA TM-87763, July 1986.

[4]Crawley, E. G., and de Luis, J., "Use of Piezo-Ceramics as Distributed Actuators in Large Space Structures," *AIAA Journal*, Vol. 25, No. 10, 1987, pp. 1373–1385.

[5]Im, S. A, and Atluri, S. N., "Effects of Piezo-Actuators on a Finitely Deformed Beam Subjected to General Loading," *AIAA Journal*, Vol. 27, No. 12, 1989, pp. 1801–1807.

[6]Thareja, R., and Haftka, R. T., "NEWSUMT-A, A Modified Version of NEWSUMT for Inequality and Equality Constraints," Virginia Polytechnic Inst. and State Univ., Blacksburg, VA, March 1985.

Partial Hybrid Strip Model for Higher-Order Laminated Plate Theory

Yi-Ping Tseng* and Wei-Jer Wang†
Tamkang University, Taiwan 25137, Republic of China

Introduction

In the displacement-based model of classical plate theory, Mindlin theory, and higher-order theories, the essential problem is the interface traction discontinuity. The difficulty can be avoided by the hybrid stress method. However, the drawbacks are the complicated formulation and expensive computational cost. Based on the modified Hillinger-Reissner principle, a three-dimensional partial hybrid stress element has been developed by Jing and Liao.[1] The hybrid model is only partially used in transverse shear part; however, excellent accuracy and fast convergence are observed.

Although the finite strip method is limited to the ply orientation, its application in cross-ply and symmetrical angle-ply laminates greatly reduces the number of variables. The present study extends the finite strip method by using the higher-order plate theory, and the partial hybrid stress method is further incorporated. It is then called the partial hybrid strip model (PHSM). Quite accurate displacement results are obtained, and the through thickness stress distributions are also in fair agreement with the existing elasticity solution.

Partial Hybrid Strip Method

The displacement field of higher-order plate theory by Lo et al.[2] is adopted

$$\begin{aligned} u(x,y,z) &= u_0(x,y) + z\theta_y(x,y) + z^2 u^*(x,y) + z^3\theta_y^*(x,y) \\ v(x,y,z) &= v_0(x,y) + z\theta_x(x,y) + z^2 v^*(x,y) + z^3\theta_x^*(x,y) \\ w(x,y,z) &= w_0(x,y) + z\theta_z(x,y) + z^2 w^*(x,y) \end{aligned} \tag{1}$$

In the finite strip method, the midplane displacements are interpolated as

$$\begin{aligned} u_0 &= \sum_{i=1}^{\text{nst}} \sum_{m=1}^{r} Y_m(y) N_i(\xi) u_{0i}, \quad v_0 = \sum_{i=1}^{\text{nst}} \sum_{m=1}^{r} Y_m'(y) N_i(\xi) v_{0i} \\ w_0 &= \sum_{i=1}^{\text{nst}} \sum_{m=1}^{r} Y_m(y) N_i(\xi) w_{0i}, \quad \theta_x = \sum_{i=1}^{\text{nst}} \sum_{m=1}^{r} Y_m'(y) N_i(\xi) \theta_{xi} \\ \theta_y &= \sum_{i=1}^{\text{nst}} \sum_{m=1}^{r} Y_m(y) N_i(\xi) w_{0i}, \quad \theta_z = \sum_{i=1}^{\text{nst}} \sum_{m=1}^{r} Y_m(y) N_i(\xi) \theta_{zi} \\ u^* &= \sum_{i=1}^{\text{nst}} \sum_{m=1}^{r} Y_m(y) N_i(\xi) u_i^*, \quad v^* = \sum_{i=1}^{\text{nst}} \sum_{m=1}^{r} Y_m'(y) N_i(\xi) v_i^* \\ w^* &= \sum_{i=1}^{\text{nst}} \sum_{m=1}^{r} Y_m(y) N_i(\xi)_x w_i^*, \quad \theta_x^* = \sum_{i=1}^{\text{nst}} \sum_{m=1}^{r} Y_m'(y) N_i(\xi) \theta_{xi}^* \\ \theta_y^* &= \sum_{i=1}^{\text{nst}} \sum_{m=1}^{r} Y_m(y) N_i(\xi) \theta_{yi}^* \end{aligned} \tag{2}$$

where nst is the nodal number per strip, r the terms of series used, $Y_m(y)$ the eigenfunction, and $N_i(\xi)$ the interpolation functions between nodal lines.

Received May 13, 1991; revision received Sept. 4, 1991; accepted for publication Sept. 6, 1991.

*Assistant Professor, Department of Civil Engineering.
†Graduate Student, Department of Civil Engineering.